

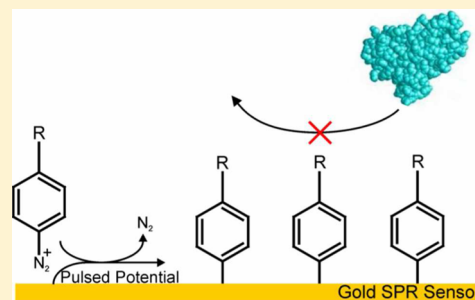
Electrografted Diazonium Salt Layers for Antifouling on the Surface of Surface Plasmon Resonance Biosensors

Qiongjing Zou, Laurel L. Kegel, and Karl S. Booksh*

Department of Chemistry and Biochemistry, University of Delaware, Newark, Delaware 19716, United States

Supporting Information

ABSTRACT: Electrografted diazonium salt layers on the surface of surface plasmon resonance (SPR) sensors present potential for a significant improvement in antifouling coatings. A pulsed potential deposition profile was used in order to circumvent mass-transport limitations for layer deposition rate. The influence of number of pulses with respect to antifouling efficacy was evaluated by nonspecific adsorption surface coverage of crude bovine serum proteins. Instead of using empirical and rough estimated values, the penetration depth and sensitivity of the SPR instrument were experimentally determined for the calculation of nonspecific adsorption surface coverage. This provides a method to better examine antifouling surface coatings and compare crossing different coatings and experimental systems. Direct comparison of antifouling performance of different diazonium salts was facilitated by a tripod SPR sensor design. The electrografted 4-phenylalanine diazonium chloride (4-APhe) layers with zwitterionic characteristic demonstrate ultralow fouling.



Development of antifouling surface coatings is crucial for surface plasmon resonance (SPR) sensing in many bioanalytical application fields, such as detection of human disease biomarkers for medical diagnostics,^{1–3} study of foodborne pathogens and toxins implicated in food safety and security,^{4–6} and hormone detection and monitoring of drug serum levels.^{7–9} A novel strategy based on electrografted diazonium salts onto gold surfaces has shown promising improvement on forming surfaces resistant to nonspecific adsorption of proteins.¹⁰ Concurrently, tethered amino acids, such as phenylalanine, have been shown to be resistant to biofouling.¹¹

Surface plasmon resonance is a well-established surface-sensitive optical technique which allows for the qualitative and quantitative measurements of biomolecular interactions in real time without requiring a labeling procedure.¹² The excellent sensitivity of SPR for detecting proteins tends the increasing popularity of SPR in bioanalyses. However, as a refractive index (RI)-based sensing technique, SPR cannot differentiate between background effects (i.e., nonspecific adsorption) and specific binding events (i.e., antigen to antibody).¹³ Nonspecific adsorption has limited applications of SPR spectroscopy for detection of biomolecules in complex matrixes (such as serum, blood, and cell lysate).⁶ Nonspecific protein interactions with the surface of biosensors create false positive responses, hindering the detection of analytes in crude biological fluids. Thus, it is necessary to reduce nonspecific adsorption, enabling the use of biosensors for direct monitoring of biomolecules in biological fluids, mitigating the need of sample cleaning steps.¹⁴

Development of coatings for protein immobilization on sensor surfaces has benefited from an extensive research history.¹⁵ Effective coatings balance the seemingly competing goals of minimizing nonspecific adsorption while introducing

reactive groups for specific immobilization.⁹ Common antifouling coatings in SPR analysis include alkanethiolate self-assembled monolayers (SAMs),¹⁶ dextran polymers,¹⁷ poly(ethylene glycol) (PEG),¹⁸ amino acids,¹⁹ and peptides.^{11,14} Chemical modification of sensor surface with alkanethiolate SAMs, taking advantage of the spontaneous formation of gold–thiol bonds, is among the most commonly used strategy for introducing surface functional groups onto SPR sensors. This easily fabricated monolayer forms a densely packed and stable structure that is oriented more or less along the normal to the metal surface.⁹ The use of short-chain thiols limits nonspecific protein adsorption to 287 ng/cm² for 16-mercaptohexadecanoic acid and 408 ng/cm² for 11-mercaptoundecanoic acid.¹⁶ Dextran polymers have shown potential to mitigate influence from interfering species in complex biological fluids. Low molecular weight (3 kDa) carboxymethyl dextran exhibits nonspecific adsorption on the order of 231 ng/cm² in serum,¹⁷ whereas the higher molecular weight dextrans, which are essential for the sensitive detection of analytes, are more prone to nonspecific bonding at the SPR surface than other coatings.^{17,20} PEG-functionalized surfaces reveal good ability for prevention of nonspecific protein adsorption with only 100 ng/cm² nonspecific adsorption.¹¹ However, their applications have been limited by the need for carboxylic acid functionalization of PEG to immobilize the molecular receptor. Bolduc et al. demonstrated that nonspecific adsorption can be substantially reduced by functionalizing gold surfaces with 3-mercaptopropionic acid (3-MPA)-linked different amino acids and peptide

Received: December 4, 2014

Accepted: December 19, 2014

Published: December 19, 2014

sequences. The concentration of nonspecifically bound proteins ranged from 416 to 808 ng/cm² for 3-MPA–amino acids,¹⁹ and to lower than 100 ng/cm² for some binary patterned peptide SAMs.¹⁴

Diazonium salts have gained popularity due their uncomplicated functionalization procedure, resulting in chemically versatile surfaces on different substrates with applications to chemical and biomolecular sensing, catalysis, and corrosion protection.²¹ Pertaining to biosensing applications and, more specifically, to the rejection of nonspecific adsorption of biomolecules, diazonium salts have been initially applied as linkers followed by attachment of the protein, or by first conjugating diazonium salt precursor to protein followed by diazotization to the perspective diazonium salt modified protein, enabling one-step attachment of bioreceptor–diazonium salt adducts,^{22–24} which can decrease nonspecific binding of proteins to the surface. Alternatively, diazonium salts have been combined with PEG to impart resistance toward nonspecific adsorption, but no chemical specificity, on glassy carbon electrodes.^{25,26} Although diazonium salts have shown great potential as an antifouling coating, an extensive evaluation of the performance in highly fouling media has not been presented.

The level of nonspecific adsorption for each coating in this study was determined by measuring the shift in resonant wavelength ($\Delta\lambda_{\text{SPR}}$) before and after exposure to crude bovine serum solutions; however, direct comparison of antifouling coating efficacy across the literature can be problematic. To obtain the nonspecific adsorption surface coverage (Γ) from $\Delta\lambda_{\text{SPR}}$

$$\Gamma = \rho \left(\frac{-l_d}{2} \right) \ln \left(1 - \frac{\Delta\lambda_{\text{SPR}}}{m(\eta_a - \eta_s)} \right) \quad (1)$$

from Jung et al.²⁷ has been employed,^{2,7,10,11,14,16,17,19} where ρ is the protein density, η_a is the refractive index of the absorbed protein, and η_s is the refractive index of the bulk solution. The effective sensing volume of SPR is defined by its electromagnetic field which decays away exponentially into the dielectric and is represented by the characteristic penetration depth (l_d).²⁸ The l_d of a surface plasmon increases with increasing wavelength of surface plasmon resonance (λ_{SPR}); at the interface between planar gold and a medium with a refractive index of 1.32 it can vary from ~ 160 nm l_d at 600 nm λ_{SPR} to ~ 260 nm l_d at 700 nm λ_{SPR} .⁹ A rough estimate of l_d as 0.37 of the wavelength (λ) was presented in Jung et al.'s work;²⁷ some simply employed 230 nm at $\lambda_{\text{SPR}} \sim 630$ nm as the estimate in all the calculations of Γ .^{2,7,11,16,17,19} As a key parameter in the calculation of Γ , l_d needs to be incorporated properly in order to assess antifouling surface coatings and provide better comparisons among different coatings and experimental systems. Therefore, a better estimate of l_d must be demonstrated. The sensitivity (m) of SPR instrument also varies with λ_{SPR} . The SPR response to bulk solutions in all cases is fairly linear over a narrow enough refractive index range but exhibits significant curvature across a broader index range.²⁷ Typically, a constant estimation of sensor sensitivity was employed for all the calculations of Γ when comparing surface coatings.^{2,7,11,16,17,19} This methodology is accurate only when the adsorption process investigated for each coating covers a similar wavelength range. If a high refractive index or thick surface coating is used, there will be a red-shift in the λ_{SPR} relative to lower RI samples. Then, using the sensitivity

determined at a shorter SPR wavelength or across a broad SPR wavelength range will lead to a biased estimation of Γ . Hence, a method to determine m that is suitable in calculation of Γ for each surface coating is needed.

The recent work by Jiang's group has demonstrated excellent resistance to nonspecific adsorption using a monolayer of a zwitterionic polymer,^{29,30} while they used a conversion of a 1 nm SPR wavelength shift representing a change in the protein surface coverage of 17 ng/cm² for quantitative estimation of surface mass coverage with the SPR sensor operating at a resonant wavelength of around 750 nm.

In this paper, employing electrografted diazonium salts on gold layers as antifouling coatings in crude bovine serum utilizing SPR spectroscopy is reported. Determination of the penetration depth and sensitivity of the SPR instrument to enable proper calculation of the nonspecific adsorption surface coverage has been demonstrated over various wavelengths in theory and in practice. Comparison of antifouling performance between diazonium salts with different functional groups is presented. The number of applied potential pulses as one important electrografting condition has been studied. Nonspecific adsorption surface coverage of alkanethiolate SAMs was also studied and compared with literature values and that of diazonium salts.

■ EXPERIMENTAL SECTION

Experimental Setup. The gold-coated slides were prepared according to the procedure previous published.^{10,31} Two sets of gold-coated slides were employed in this study. One set of slides was coated with uniform gold covering the whole slides. The second set contained three gold sensing pads separated by 3 mm. (See the Supporting Information for detailed procedure.) Spectroscopic measurements were acquired on an electrochemical SPR instrument with a dove prism previously described.³¹ (See the Supporting Information for detailed procedure.)

Sensor Modification Procedure. Three diazonium salts, 4-phenylalanine diazonium chloride (4-APhe), 4-phenylacetic diazonium chloride (4-PAD), and 4-nitrobenzene diazonium tetrafluoroborate (4-NDT, Sigma-Aldrich), were studied. Except for 4-NDT, which was commercially available, 4-APhe and 4-PAD were generated in situ from their precursors, respectively, 4-amino-DL-phenylalanine hydrate (97%, Acros Organics) or 4-aminophenylacetic acid (98%, Acros Organics), according to the procedure previous published.^{10,31} (See the Supporting Information for detailed procedure.) The diazonium salt solutions were then immediately used to perform electrografting by syringe injecting the solution into the 180 μ L electrochemical flow cell. Diazonium salt layers on SPR sensor surfaces were obtained by electrografting, the procedure of which consisted of applying a series of 2 s, negative potential pulses to the designated SPR sensing pad. Potentials applied were -550 mV for 4-APhe and -400 mV for 4-PAD and 4-NDT. The number of pulses, 1, 5, 10, and 20, was evaluated.

Alkanethiolate self-assembled monolayers (HS-(CH₂)_xCOOH, $x = 2, 10, 15$) were formed on freshly sputtered gold-coated slides by immersion overnight in solution of 10 mM 3-mercaptopropionic acid (3-MPA, 99+%, Acros Organics), 5 mM 11-mercaptoundecanoic acid (11-MUA, 95+%, Santa Cruz Biotechnology), or 5 mM 16-mercaptohexadecanoic acid (16-MHA, 99+%, Asemblon Inc.) in absolute ethanol. Just before mounting the slides on the electrochemical SPR instrument, the samples were rinsed with copious amounts

of ethanol and deionized water and dried with a nitrogen gas stream. Also, a 3-mercaptopropyl-phenylalanine (3-MPA-Phe) monolayer was prepared by employing the widely used carbodiimide coupling reaction.³² A solution containing 100 mM *N*-(3-(dimethylamino)propyl)-*N'*-ethylcarbodiimide (EDC, 99%, Sigma-Aldrich) and 25 mM *N*-hydroxysuccinimide (NHS, 98%, Fisher Scientific) was injected to the flow cell and stopped atop 3-MPA monolayer for 20 min, followed by deionized water flushing. Then, a solution of 10 mM L-phenylalanine (Phe, 98.5+%, Acros Organics) in phosphate-buffered saline (PBS, pH 7.4, MP Biomedicals) was injected and allowed to react for 30 min to form 3-MPA-Phe monolayer, followed by PBS flushing.

Nonspecific Binding Monitoring. Once the SPR sensors with different surface coatings were prepared and mounted on the electrochemical SPR instrument, the flow cell was flushed with several milliliters of PBS. SPR spectra were collected real time over a 5 min period in PBS, followed by a 20 min of exposure to undiluted bovine serum (Sigma-Aldrich) containing 75 mg/mL proteins and a subsequent 5 min PBS washing step to remove weakly adsorbed species.¹⁹ The level of nonspecific adsorbed proteins on each modified surface was determined by measuring the shift in resonant wavelength before and after exposure to bovine serum. The data acquisition was performed at a rate of 1 data point every 5 s using 1200 g/mm grating with 0.058 nm resolution. Raw data were then processed with MatLab software. This procedure along with surface modification was repeated at least three times on new gold-coated slides for each type of surface coating.

RESULTS AND DISCUSSION

Surface Modification by Diazonium Salts. Surface modification by electrografting diazonium salts on gold surfaces is realized by pulsed potential profile, which is also referred to as pulsed chronoamperometry. Electrografting procedure of 4-APhe, as an example, is evident in Figure 1. A series of 2 s,

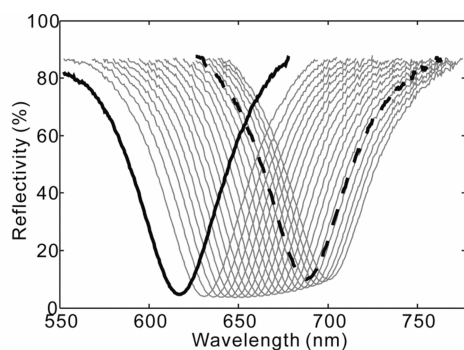


Figure 1. SPR curves of 4-APhe modification by 20 pulses attachment. SPR curve in water before surface modification (black solid line), SPR curves in 4-APhe solution after each 2 s, -550 mV pulse (gray solid lines), and SPR curve in water after surface modification (black dashed line).

negative potential pulses were applied on the SPR sensing pad for electrochemical reduction and deposition of the diazonium salts on gold. A “rest” period (10 s) following each pulse allowed pausing the reduction process and replenishment of the diazonium salt within the depletion layer. A red-shift of the resonant wavelength (gray solid lines) after each pulse demonstrated 4-APhe gradually electrografted on gold. After 20 pulses, a large $\Delta\lambda_{\text{SPR}}$ (~ 70 nm) was observed between two

SPR curves (black dashed and black solid lines) in water. The previous work revealed that, compared to the conventional electrochemical techniques (i.e., potentiostatic and cyclic voltammetry), pulsed profiles have shown more compact and uniformly distributed layers over the surface.¹⁰ The same manner of surface modification was employed for the other two diazonium salts, 4-PAD and 4-NDT. Additionally, number of pulses, as one important electrografting condition in terms of nonspecific proteins adsorption, was studied across the range of 1–20 pulses.

Individual functionalization of different diazonium salts on separate pads in the same fluidic channel was facilitated by a tripad SPR sensor design that enabled simultaneous monitoring and direct comparison of three surfaces exposed to one solution. (See Scheme S-1 in the Supporting Information.) At time 2 min, the diazonium salt solution (4-PAD in Figure 2A or

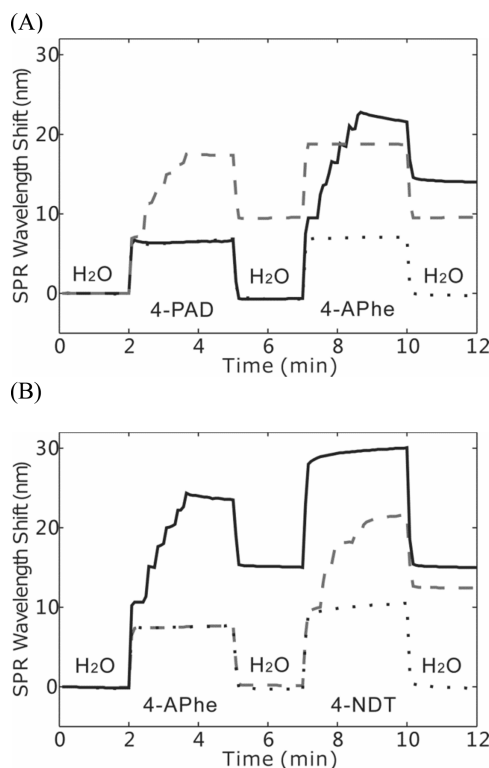


Figure 2. SPR sensorgrams of individual modifications of different diazonium salts on separate pads in the same fluidic channel on a tripad SPR sensor. Five clear steps between 2 and 5 min and 7–10 min demonstrate the electrografting of diazonium salt to the designated pad. (A) 4-APhe (black solid line), bare gold (black dotted line), and 4-PAD (gray dashed line). (B) 4-APhe (black solid line), bare gold (black dotted line), and 4-NDT (gray dashed line).

4-APhe in Figure 2B) was injected into the water-filled flow cell and a concomitant red-shift in the resonance wavelength was observed due to the refractive index increasing from water to the diazonium salt solution. Then, a series of five pulses were applied to only one of the three SPR pads (gray dashed line in Figure 2A or black solid line in Figure 2B). Five clear steps demonstrate the electrografting of diazonium salt to the designated pad. At the 5 min mark, water was injected into the flow cell. Then, the working electrode was switched to connect another SPR pad (black solid line in Figure 2A or gray dashed line in Figure 2B), and at time 7 min the flow cell was subsequently filled with a different diazonium salt solution (4-

APhe in Figure 2A or 4-NDT in Figure 2B). Another series of five pulses were applied to that pad, and five clear steps were observed from the designated SPR pad. At the 10 min mark, water was injected into the flow cell again. An SPR wavelength increasing between water steps was only observed on the SPR pad with applied potential pulses. The SPR signal from other pads only responded to refractive index changes associated with the injected solutions and returned to the water baseline at the washing step. At the end, two SPR pads (black solid and gray dashed lines) were individually functionalized with difference diazonium salts, and the bare gold pad (black dotted lines) was left as unaffected.

Determination of Penetration Depth. As a key parameter in the calculation of Γ , penetration depth (l_d) needs to be incorporated properly for characterization of antifouling surface coatings. As demonstrated in eq 1, Γ is derived from l_d ; therefore, incorporating a proper l_d estimate is important for determination of Γ , especially when Γ is fairly low.

There are a few different methods that can be used to estimate l_d . An empirical rough estimate of l_d as 0.37λ ²⁷ has been used to calculate Γ .^{2,7,11,16,17,19} A more proper estimate of l_d comes from the Maxwell's equations,²⁸ theoretically:

$$l_d = \frac{\lambda}{2\pi} \sqrt{\frac{\epsilon_m' + \epsilon_s}{\epsilon_s^2}} \quad (2)$$

where ϵ_m' is the real part of the complex dielectric constant of the metal, specifically gold in here, and ϵ_s is the dielectric constant of the bulk solution, specifically PBS in here. ϵ_m' can be given by

$$\epsilon_m' = \eta_m^2 - k_m^2 \quad (3)$$

where the values of refractive index of gold (η_m) and extinction coefficient of gold (k_m) both varying by wavelength can be found from *Handbook of Optical Constants of Solids*³³ or Johnson and Christy.³⁴ Since the extinction coefficient of bulk solution is negligible ($<1 \times 10^{-7}$), $\epsilon_s = \eta_{\text{PBS}}^2$, where η_{PBS} was determined experimentally with a refractometer at 1.334.

Recent work has shown determination of l_d experimentally with great consistency and agreement with theory over a wavelength range of $\lambda = 701\text{--}1152\text{ nm}$.³⁵ l_d can be estimated by fitting the experimental values of l_d (nm) from that work as a function of λ (nm) into a second-order polynomial equation

$$l_d = 0.0006\lambda^2 + 0.1247\lambda - 123.01 \quad (4)$$

which provides a good way to assess l_d from difference methods.

A comparison of l_d determined by the methods mentioned shows qualitative agreement, although the empirical rough estimate of l_d as 0.37λ rapidly diverges from the other values in the near-infrared (Figure 3). Empirical l_d estimated by 0.37λ is only accurate around 700 nm wavelength. Given the wavelength range of 620–685 nm investigated in this work, among the rest of the three curves, the middle values (black squares with black dashed line) presented method, that is by Maxwell's equations with η_m and k_m values from Johnson and Christy, was employed for the following calculation of l_d . Theoretical l_d was calculated by this method at specific wavelength for every modified surface and incorporated in the calculation of nonspecific adsorption surface coverage.

Determination of the Sensitivity of the SPR Instrument. As another key parameter varying by wavelength in the

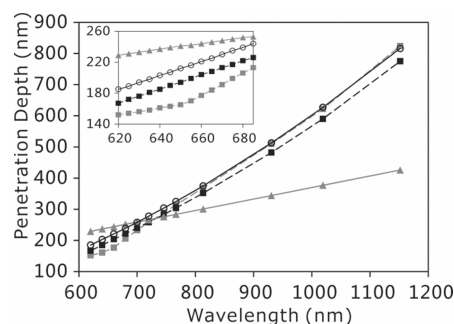


Figure 3. Comparison of penetration depth determined by different methods. Empirical l_d calculated by 0.37λ (gray triangles with gray solid line), theoretical l_d calculated by Maxwell's equations with η_m and k_m values from *Handbook of Optical Constants of Solids* (gray squares with gray dashed line) and Johnson and Christy (black squares with black dashed line), and l_d calculated by experimental values fitted with eq 4 (open circles with black solid line). Inset is a zoom-in on the wavelength range of 620–685 nm.

calculation of Γ , the sensitivity (m) of SPR instrument needs to be determined properly. Typically, m is measured by the slope of a calibration plot of SPR wavelength (λ_{SPR}) as a function of refractive index (η) of the bulk solution in contact with the sensor surface. SPR wavelength shift is fairly linear over a narrow enough refractive index range but exhibits significant curvature across a broader index range.²⁷ The curvature in such calibration plot can be explicitly incorporated into a second-order polynomial equation²⁷ as

$$\lambda_{\text{SPR}} = m_1\eta^2 + m_2\eta + b \quad (5)$$

where $m_2\eta^2$ can only be negligible for a very small $\Delta\eta$.

An m at specific wavelength in each calculation of Γ needs to be determined, because using the same m calculated by $\Delta\lambda_{\text{SPR}}/\Delta\eta$ from the linear relationship will lead to a biased estimation of Γ , when the wavelength investigated for each adsorption process was neither similar nor narrow enough. Additionally, bulk sensitivity remains statistically similar regardless of functionalization on the sensor surface,³⁵ hence, m values for bare gold can be used. The SPR resonant wavelength was observed as a function of refractive index for five NaCl standard solutions over bare gold (the refractive indices were 1.3330, 1.3418, 1.3505, 1.3594, and 1.3684, corresponding to mass concentration of 0.00%, 5.00%, 10.00%, 15.00%, and 20.00%³⁶). (See Figure S-1 in the Supporting Information.) As shown in eq 5, a second-order polynomial fit to λ_{SPR} (nm) as a function of η (RIU, refractive index unit) could be obtained as

$$\lambda_{\text{SPR}} = 18682\eta^2 - 48320\eta + 31834 \quad (6)$$

Therefore, m can be estimated with a narrow enough $\Delta\lambda_{\text{SPR}}$ (20 nm) divided by corresponding $\Delta\eta$. The η values could be solved in eq 6 by inputting specific λ_{SPR} values (five λ_{SPR} values used with 5 nm interval) that are similar to the nonspecific adsorption process investigated.

This methodology was verified by comparing estimated m values with experimental m values over various wavelengths (Table 1). Given the small difference ($\leq \pm 2.5\%$) between the experimental and estimated m values over λ_{SPR} range from narrow (15 nm) to broad (77 nm), estimated m values can be used as good substitutes for m values in the following calculation of Γ . Also, estimated m varying from 1721.0 nm/RIU for λ_{SPR} range of 620–640 to 2522.4 nm/RIU for λ_{SPR} range of 665–685 nm was noticed, which revealed the

Table 1. Comparison of Experimental and Estimated Sensitivity (m)

λ_{SPR} range (nm) ^a	exptl m (nm/RIU)	estimated m (nm/RIU)	difference from exptl values (%)
620–635	1721.8	1678.6	–2.5
635–697	2302.6	2338.5	1.6
620–697	2149.1	2169.1	0.93

^aEach with 4–6 evenly dispersive data points.

importance of including the proper m in the determination of Γ .

Nonspecific Adsorption of Serum Proteins on Modified Surfaces. The level of nonspecific adsorption on each modified surface coating was evaluated by measuring the $\Delta\lambda_{\text{SPR}}$ before and after exposure to crude bovine serum and further quantified as the nonspecific adsorption surface coverage (Γ). Simultaneous monitoring and direct comparison of $\Delta\lambda_{\text{SPR}}$ on 4-APhe and another two diazonium salt (4-PAD and 4-NDT) modified pads in the same fluidic channel were facilitated by a tripad SPR sensor design (Figure 4). With five

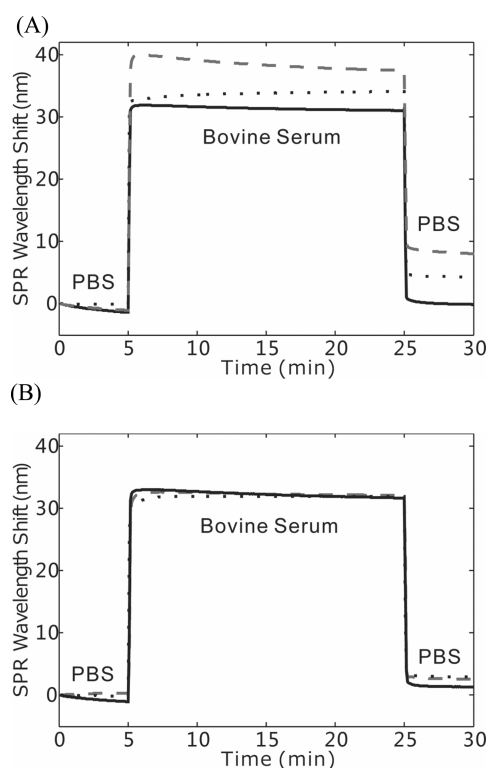


Figure 4. SPR sensorgrams of different diazonium salts (4-APhe and 4-PAD in panel A, 4-NDT in panel B) modified tripad SPR sensor surfaces exposed to bovine serum for simultaneous monitoring and direct comparison nonspecific adsorption of proteins. (A) 4-APhe (black solid line), bare gold (black dotted line), and 4-PAD (gray dashed line). (B) 4-APhe (black solid line), bare gold (black dotted line), and 4-NDT (gray dashed line).

pulses electrografting modification, 4-APhe-modified surfaces displayed the best performance on resistance to nonspecific adsorption of bovine serum proteins, in comparison to another two diazonium salts and bare gold. After the tripad sensors were modified as demonstrated in Figure 2, the sensors were stabilized for 5 min in PBS, followed by a 20 min exposure to undiluted bovine serum and a subsequent 5 min PBS washing

step. Red-shifted $\Delta\lambda_{\text{SPR}}$ was observed before and after exposure to bovine serum; 4-APhe-modified surfaces (black solid lines in Figure 4) demonstrated much less $\Delta\lambda_{\text{SPR}}$ compared to 4-PAD-modified surface (gray dashed line in Figure 4A), 4-NDT-modified surface (gray dashed line in Figure 4B), and bare gold (black dotted lines in Figure 4).

Electrografting of the three diazonium salts was further optimized by determining the best number of pulses to minimize surface fouling by bovine serum (Figure 5). Equation

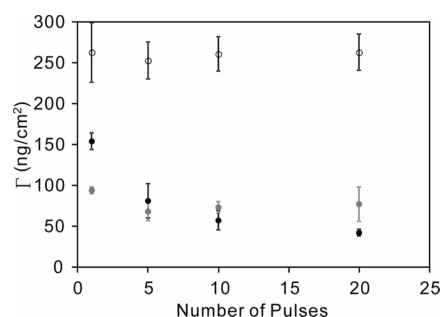


Figure 5. Nonspecific adsorption surface coverage (Γ) of bovine serum as a function of number of pulses for three different diazonium salts: 4-APhe (black solid dots), 4-PAD (black empty dots), and 4-NDT (gray solid dots). The error bars depict standard deviations of the mean of three measurements from three individual samples.

1 was employed to calculate Γ from $\Delta\lambda_{\text{SPR}}$. l_d and m were determined from the methods discussed above. Protein density (ρ) of 1.3 g/mL, the refractive index of the adsorbed protein (η_a) of 1.57,²⁷ and the refractive index of the bulk solution (η_s) of 1.334 were employed for the calculations as mentioned above. When these three diazonium salt layers are compared, 4-APhe showed excellent performance for resistance to nonspecific adsorption of proteins, especially at a greater number of pulses, and 4-NDT also showed good ability of resistance to nonspecific adsorption of proteins, especially at lower number of pulses.

Binding of water molecules by the antifouling layers is important in their ability to resist protein adsorption; if the interfering protein cannot easily displace water, it cannot interact, and adsorb, onto the organic layer.^{37,38} Upon consideration of this surface immobilization mechanism, it becomes apparent that the different functional groups at the surfaces of electrografted diazonium salt layers affect their antifouling performance greatly. The primary amine and carboxylic acid groups on the top of 4-APhe present a zwitterionic state at physiological pH. Zwitterions form a hydration layer via electrostatic interactions and are capable of binding a significant amount of water molecules.³⁸ Also, it should be noticed that, for 4-APhe, as the number of pulses increases, lower and more stable Γ was observed. The explanation could be the higher number of pulses produced more complete and uniformly distributed layers over the surface. Previous work has shown that electrografted diazonium salts form disordered, multilayered polyphenylene networks growing from nodular aggregates.^{39,40} Ellipsometric analysis of the 4-phenylalanine adlayers shows an increasing average thickness from ~ 1.1 nm with one pulse to ~ 24 nm with 20 pulses.¹⁰ The thicker layers, hence, better present a hydrated, zwitterionic network that is free of holes and shielded from surface effects at the gold interface that may lead to increased probability of fouling.

In contrast to 4-APhe, Γ for 4-PAD is ~ 260 ng/cm² at all number of pulses studied, since 4-PAD only has carboxylic acid groups on the top, which are easily deprotonated and form negative net charges. Surfaces with net charges are prone to interact with proteins, rendering them more susceptible to nonspecific adsorption. The electrically neutral nitro groups on the top of 4-NDT are less likely to interact with proteins, but the hydrophobic property of nitrobenzene makes it less favorable for antifouling. Therefore, at lower number of pulses, 4-NDT presents low fouling. However, as the number of pulses increases (e.g., 20 pulses) the multilayered nitrobenzene network grows, which makes the 4-NDT layers more favorable for fouling. Hence, the number of pulses should be wisely chosen to achieve optimal antifouling performance. Also, the application of 4-NDT as an antifouling surface coating was limited by the need for introducing reactive groups for specific immobilization, while carboxylic acid groups of 4-APhe or 4-PAD can easily immobilize proteins by employing the widely used carbodiimide coupling reaction.³²

The antifouling ability of more conventional approaches relying on alkanethiolate SAMs and 3-MPA linked phenylalanine (3-MPA-Phe) was studied on the same experimental system and compared with that of diazonium salt layers (Table 2). The diazonium salt, 4-APhe, demonstrated the best

Table 2. Nonspecific Adsorption Surface Coverage (Γ) of Bovine Serum on Diazonium Salts and Alkanethiolate Monolayers^a

antifouling surface coatings	Γ (ng/cm ²) ^b
4-APhe (20 pulses)	42 \pm 4
4-NDT (5 pulses)	68 \pm 11
bare gold	96 \pm 2
3-MPA	229 \pm 31
11-MUA	233 \pm 52
16-MHA	237 \pm 7
4-PAD (5 pulses)	253 \pm 23
3-MPA-Phe	409 \pm 102

^aMeasurements in triplicate and the error represent standard deviations of the mean. ^bCalculated with l_d from Maxwell's equations with η_m and k_m values from Johnson and Christy.

antifouling performance, with 5–10-fold improvement over other surface coatings. The three alkanethiolate SAMs with different chain lengths (3-MPA, 11-MUA, and 16-MHA) presented very similar Γ values as 4-PAD, and all these four coatings have only carboxylic acid groups at the top, which further confirmed that the functional groups at the top of the surface coatings are crucial for antifouling. Unlike the zwitterionic characteristic of 4-APhe, the resulting SAM of 3-MPA-Phe, by coupling 3-MPA to the phenylalanine through the amine group, displayed hydrophobic and anionic characteristics from the aromatic side chain and the carboxylate group, rendering it more susceptible to nonspecific adsorption. Fouling on bare gold was between that on diazonium salts (4-APhe and 4-NDT) and alkanethiolate SAMs over 20 min of exposure to the bovine serum. However, gold shows a higher tendency for spontaneous adsorption of proteins over longer time,^{41,42} and this passive binding to the metal substrate results in a loss of the bioactivity.⁹ Finally, nonspecific adsorption surface coverage values in this work were compared with the available data in literature (Table 3). Incorporating the theoretical l_d or empirical l_d could vary Γ by $\sim 25\%$ (Table 3,

Table 3. Comparison of Nonspecific Adsorption Surface Coverage (Γ) Values in This Work (Measurements in Triplicate, and the Error Represents Standard Deviations of the Mean) with Literature Values

antifouling surface coatings	Γ (ng/cm ²) ^a	Γ (ng/cm ²) ^b	Γ_{lit} (ng/cm ²) ^b
4-APhe (20 pulses)	42 \pm 4	44 \pm 4	N/A
4-APhe (5 pulses)	81 \pm 21	108 \pm 27	62 \pm 21 ^c
11-MUA	233 \pm 52	307 \pm 68	408
16-MHA	237 \pm 7	315 \pm 9	287
3-MPA-Phe	409 \pm 102	550 \pm 137	575 \pm 202

^aCalculated with l_d from Maxwell's equations with η_m and k_m values from Johnson and Christy. ^bCalculated with empirical l_d , which is estimated by 0.37λ as 230 nm. ^cNonspecific adsorption of 76 mg/mL bovine serum albumin, instead of crude bovine serum.

columns 2 and 3). If the same l_d was employed, given the variance of instrumental systems and bovine serum samples, our results were consistent with the results in literature (Table 3, columns 3 and 4).

CONCLUSIONS

In this paper, electrografted diazonium salts as antifouling surface coatings in crude bovine serum on SPR gold sensors were investigated. Determination of the proper penetration depth and sensitivity of SPR instrument was demonstrated. The importance of incorporating the proper penetration depth and SPR sensitivity in the determination of nonspecific adsorption surface coverage and assessment antifouling surface coatings was discussed. Comparison antifouling performance between diazonium salts with different functional groups and alkanethiolate self-assembled monolayers was presented. The diazonium salt of 4-APhe electrografted with 20 pulses exhibited the best potential on antifouling by reducing the nonspecific adsorption surface coverage down to 42 ± 4 ng/cm². The dramatic improvement of 4-APhe layers over other antifouling surface coatings can be explained by the retention of the zwitterionic characteristics of electrografted 4-APhe.

ASSOCIATED CONTENT

Supporting Information

Additional information as noted in text. This material is available free of charge via the Internet at <http://pubs.acs.org>.

AUTHOR INFORMATION

Corresponding Author

*Phone: +1 302-831-2561. Fax: +1 302-831-6335. E-mail: kbooksh@udel.edu.

Notes

The authors declare no competing financial interest.

ACKNOWLEDGMENTS

Funding from the National Institutes of Health is acknowledged through Grant No. R01EB0044761.

REFERENCES

- (1) Liu, J. T.; Chen, C. J.; Ikoma, T.; Yoshioka, T.; Cross, J. S.; Chang, S. J.; Tsai, J. Z.; Tanaka, J. *Anal. Chim. Acta* **2011**, 703, 80–86.
- (2) Masson, J. F.; Battaglia, T. M.; Khairallah, P.; Beaudoin, S.; Booksh, K. S. *Anal. Chem.* **2007**, 79, 612–619.
- (3) Noguez, C.; Leh, H.; Langendorf, C. G.; Law, R. H. P.; Buckle, A. M.; Buckle, M. *PLoS One* **2010**, 5, DOI: 10.1371/journal.pone.0012152.

- (4) Chen, L.; Zeng, R.; Xiang, L.; Luo, Z.; Wang, Y. *Anal. Methods* **2012**, *4*, 2852–2859.
- (5) Rodriguez-Emmenegger, C.; Avramenko, O. A.; Brynda, E.; Skvor, J.; Alles, A. B. *Biosens. Bioelectron.* **2011**, *26*, 4545–4551.
- (6) Shankaran, D. R.; Gobi, K. V. A.; Miura, N. *Sens. Actuators, B* **2007**, *121*, 158–177.
- (7) Battaglia, T. M.; Masson, J. F.; Sierks, M. R.; Beaudoin, S. P.; Rogers, J.; Foster, K. N.; Holloway, G. A.; Booksh, K. S. *Anal. Chem.* **2005**, *77*, 7016–7023.
- (8) Danelian, E.; Karlen, A.; Karlsson, R.; Winiwarter, S.; Hansson, A.; Lofas, S.; Lennernas, H.; Hamalainen, M. D. *J. Med. Chem.* **2000**, *43*, 2083–2086.
- (9) Homola, J. *Surface Plasmon Resonance Based Sensors*; Springer-Verlag: Berlin, Germany, 2006.
- (10) Menegazzo, N.; Zou, Q.; Booksh, K. S. *New J. Chem.* **2012**, *36*, 963–970.
- (11) Bolduc, O. R.; Clouthier, C. M.; Pelletier, J. N.; Masson, J. F. *Anal. Chem.* **2009**, *81*, 6779–6788.
- (12) Hoa, X. D.; Kirk, A. G.; Tabrizian, M. *Biosens. Bioelectron.* **2007**, *23*, 151–160.
- (13) Boozer, C.; Yu, Q. M.; Chen, S. F.; Lee, C. Y.; Homola, J.; Yee, S. S.; Jiang, S. Y. *Sens. Actuators, B* **2003**, *90*, 22–30.
- (14) Bolduc, O. R.; Pelletier, J. N.; Masson, J. F. *Anal. Chem.* **2010**, *82*, 3699–3706.
- (15) Yebra, D. M.; Kiil, S.; Dam-Johansen, K. *Prog. Org. Coat.* **2004**, *50*, 75–104.
- (16) Masson, J.-F.; Battaglia, T. M.; Cramer, J.; Beaudoin, S.; Sierks, M.; Booksh, K. S. *Bioanal. Chem.* **2006**, *386*, 1951–1959.
- (17) Masson, J. F.; Battaglia, T. M.; Davidson, M. J.; Kim, Y. C.; Prakash, A. M. C.; Beaudoin, S.; Booksh, K. S. *Talanta* **2005**, *67*, 918–925.
- (18) McPherson, T.; Kidane, A.; Szleifer, I.; Park, K. *Langmuir* **1998**, *14*, 176–186.
- (19) Bolduc, O. R.; Masson, J.-F. *Langmuir* **2008**, *24*, 12085–12091.
- (20) Frazier, R. A.; Matthijs, G.; Davies, M. C.; Roberts, C. J.; Schacht, E.; Tandler, S. J. B. *Biomaterials* **2000**, *21*, 957–966.
- (21) Belanger, D.; Pinson, J. *Chem. Soc. Rev.* **2011**, *40*, 3995–4048.
- (22) Corgier, B. P.; Bellon, S.; Anger-Leroy, M.; Blum, L. J.; Marquette, C. A. *Langmuir* **2009**, *25*, 9619–9623.
- (23) Corgier, B. P.; Marquette, C. A.; Blum, L. J. *Biosens. Bioelectron.* **2007**, *22*, 1522–1526.
- (24) Corgier, B. P.; Marquette, C. A.; Blum, L. J. *J. Am. Chem. Soc.* **2005**, *127*, 18328–18332.
- (25) Khor, S. M.; Liu, G. Z.; Fairman, C.; Iyengar, S. G.; Gooding, J. *J. Biosens. Bioelectron.* **2011**, *26*, 2038–2044.
- (26) Liu, G. Z.; Gooding, J. J. *Langmuir* **2006**, *22*, 7421–7430.
- (27) Jung, L. S.; Campbell, C. T.; Chinowsky, T. M.; Mar, M. N.; Yee, S. S. *Langmuir* **1998**, *14*, 5636–5648.
- (28) Schasfoort, R. B. M.; Tudos, A. J. *Handbook of Surface Plasmon Resonance*; RSC Publishing: Cambridge, U.K., 2008.
- (29) Huang, C. J.; Li, Y. T.; Jiang, S. Y. *Anal. Chem.* **2012**, *84*, 3440–3445.
- (30) Vaisocherova, H.; Zhang, Z.; Yang, W.; Cao, Z. Q.; Cheng, G.; Taylor, A. D.; Piliarik, M.; Homola, J.; Jiang, S. Y. *Biosens. Bioelectron.* **2009**, *24*, 1924–1930.
- (31) Zou, Q.; Menegazzo, N.; Booksh, K. S. *Anal. Chem.* **2012**, *84*, 7891–7898.
- (32) Grabarek, Z.; Gergely, J. *Anal. Biochem.* **1990**, *185*, 131–135.
- (33) Palik, E. D. *Handbook of Optical Constants of Solids*; Academic Press: San Diego, CA, 1985.
- (34) Johnson, P. B.; Christy, R. W. *Phys. Rev. B* **1972**, *6*, 4370–4379.
- (35) Kegel, L. L.; Menegazzo, N.; Booksh, K. S. *Anal. Chem.* **2013**, *85*, 4875–4883.
- (36) Mettler-Toledo Web site. <http://www.mt.com/> (accessed February 07, 2012).
- (37) Harder, P.; Grunze, M.; Dahint, R.; Whitesides, G. M.; Laibinis, P. E. *J. Phys. Chem. B* **1998**, *102*, 426–436.
- (38) Chen, S. F.; Zheng, J.; Li, L. Y.; Jiang, S. Y. *J. Am. Chem. Soc.* **2005**, *127*, 14473–14478.
- (39) Brooksby, P. A.; Downard, A. J. *J. Phys. Chem. B* **2005**, *109*, 8791–8798.
- (40) Kariuki, J. K.; McDermott, M. T. *Langmuir* **1999**, *15*, 6534–6540.
- (41) Anand, G.; Jamadagni, S. N.; Garde, S.; Belfort, G. *Langmuir* **2010**, *26*, 9695–9702.
- (42) Castner, D. G.; Ratner, B. D. *Surf. Sci.* **2002**, *500*, 28–60.